

# Pore Pressure Response of Undrained Two-Way Cyclic Loading of Silt

Aminaton Marto, Ph.D

Department of Geotechnics and Transportation  
Faculty of Civil Engineering  
Universiti Teknologi Malaysia

## ABSTRACT

A series of stress-controlled undrained two-way cyclic loading tests were performed on reconstituted samples of isotropically consolidated Keuper Marl silt (LL = 36%, PI = 19%) of various stress histories and stress levels. The series included cyclic loading with and without rest-periods, and resulted in either failure or non-failure of the sample during cyclic loading. Following a rest-period, non-failure samples were subject to further cyclic loading. Studies on the pore pressure response of normally consolidated samples indicated that permanent pore pressure developed steadily with the loading period, but the rate of development decreased as the loading period increased. A linear relationship was found to exist between the normalised permanent pressure rate and time, plotted on logarithmic scales.

## INTRODUCTION

It is a commonly held view that, under cyclic loading, pore water pressure and permanent strain build up, and the soil's elastic modulus degrades [1]. Failure due to cyclic loading will occur when either (i) pore pressure accumulation reduces the effective stresses to a critical level or (ii) greater permanent strains are produced than those the foundation was designed to accommodate. However, it must be stressed that cyclic loading will not always lead to failure. In fact it may occasionally have beneficial effects such as when the dissipation of the pore pressure takes place during rest-periods in between the cyclic loading. Brown et. al. [2] and later, Yasuhara [3] found that drainage after cyclic loading has a significant strengthening effect for normally consolidated clay. In addition low pore pressures are generated during subsequent cyclic loading.

Laboratory results by previous researchers [4],[5] show that this pore pressure response comprise of two different components; cyclic or resilient pore water pressure and permanent or mean pore water pressure (Fig. 1).

### **Permanent Pore Water Pressure**

From Fig. 1, it can be seen that pore water pressure will increase to a maximum value as the cyclic stress reaches its maximum level, then decreases as the cyclic stress is released. So if the soil is subjected to cyclic loading for sometime then stopped, the pore water pressure will have a residual value after the cyclic stress has stopped. In other words, this pore water pressure termed as permanent or mean pore water pressure, is an important aspect in analysing the response of soil under cyclic loading because it will stay in the soil after the cyclic loading ends. However, if the cyclic loading continues or the cyclic stress level imposed is high enough, the permanent pore water pressure will increase to such a level that it is equal to the applied total stress. This condition of zero effective stress is termed "liquefaction", the condition where the soil will change from solid to liquid state [6] and therefore causing failure to the overlying structures. Luong (1979) in Wood [7] summarised different phenomena observed in cyclic loading tests on sand due to the development of permanent pore water. In the undrained cyclic loading test, cycling below a characteristic state line will produce positive pore pressures, the effective stress state will migrate toward the characteristic state and small deformations may be expected. Once the characteristic state line is crossed, the tendency for dilation will result in stabilisation of the pore pressure generation, but large deformations and pore pressure variations may be expected. If the peak deviator stress does not exceed its critical state value, which is related to the specific volume and thus fixed in an undrained test, then a state of cyclic mobility may be attained with large but limited deformations [8].

The work from Sangrey [9] showed that contractive sands and clays are both susceptible to an effective stress failure created by the generation of pore pressure, although the magnitude of repeated loading required to cause failure is higher for clay than for sand. For dilative clays, he found that negative pore pressures were generated during cyclic loading and hence an effective stress failure would not occur. However, this was not true for tests on dense sand where positive pore pressures were generated. Dilative non-plastic silt was seen to behave similarly to sand but the accumulations of pore pressure occurred at a much slower rate.

Koutsoftas [1], noted that during cyclic loading, the reduction in effective stress due to excess pore pressure led to loss in undrained shear strength. However, Lee and Focht [10] found that the generation of permanent pore water pressure is fundamentally a strain dependent process. As grain contacts fail, part of the stress taken by the contact is taken by the pore water pressure causing an increase in pressure.

The work by Wilson and Greenwood [11] showed that the permanent pore pressure developed is proportional to the plastic strain and the recoverable component proportional to the elastic strain, but with a different constant of proportionality.

Hyde and Ward [12], Conn [13] and Hyde et al. [14], observed that pore water pressure increases with increasing number of cycles or time. The rate at which the pore pressure increased was seen to be a function of cyclic stress level and stress history of the soil. They concluded that under undrained cyclic loading, permanent pore pressure will develop that moves the effective stress state towards a failure condition. The number of cycles required to do this decreased with increasing cyclic deviator stress level.

### **Cyclic Pore Pressure**

Cyclic pore pressure is the difference between the maximum pore pressure and minimum pore pressure developed during each cycle of load, Figure 1. Cyclic pore pressures varied in phase with stress and, if equilibrium was reached, then the change of pore pressure was one third of the deviator stress,  $q$ , (under constant confining stress conditions) [15,16]. This indicates that the effective normal stress,  $p'$ , remains unchanged during a cycle since  $p' = q/3 + \sigma'_3$ . Raybould [5], working on a mixture of silt and clay observed that the cyclic pore pressures are approximately proportional to the applied deviator stress and are generally independent of the number of applied load cycles.

## **MATERIAL AND TEST PROCEDURES**

The material used in this research was Keuper Marl silt, and prepared as described by Marto [17] and Hyde et. al. [18]. Samples, sized 38 mm x 76 mm, were produced using one-dimensional consolidation moulds shown in Fig. 2. The equipment used for the undrained two-way cyclic loading was a computer controlled triaxial testing system based on Bishop and Wesley's stress path cell called a Geotechnical Digital System (GDS) [19], and supported by the software called GDSTTSV7 supplied by the GDS manufacturer. The GDSTTSV7 provided computer control of testing with data logging, data reduction into working units, and data presentation. The triaxial cell was linked to the computer via three microprocessor controlled hydraulic actuators called 'digital controllers' and a digital pressure interface (DPI). The controllers regulated pressure and volume change of deaerated water supplied to the cell for controlling axial load or axial deformation, cell pressure and back pressure. The system also measures axial deformation indirectly by volume change of the lower chamber of the cell. Pore pressures were measured by a solid state pressure transducer plumbed directly into the base pedestal.

The digital controllers, pore pressure, axial deformation and axial force interfaces, and printer and plotter were connected via interface bus cables to an IEEE-488 standard parallel interface of the computer [20].

The test series, shown in Table 1 and 2 are for cyclic loading tests with and without rest-periods. The tests were based on sinusoidal wave form with cyclic period of 864 seconds. The loading sequence during the tests is shown in Fig. 3.

## RESULTS AND ANALYSIS

The results showed that the two-way cyclic loading tests generates typical two-component pore pressure response, as expected, shown in Fig. 4. The responses are cyclic or resilient response and permanent response. For the cyclic response, the pore pressure varied with applied cyclic load and stress history. The parameter  $A_c$  can therefore be used to describe the cyclic pore pressure response, where  $A_c$  is simply the ratio of cyclic pore pressure to cyclic deviator stress :

$$A_c = \frac{\Delta u_c}{2q_c} \quad (1)$$

where  $\Delta u_c$  is the average peak to peak pore pressure and  $2q_c$  is the peak to peak cyclic deviator stress. The  $A_c$  values for all tests are presented in Table 3. The values varies from 0.165 to 0.386.

The permanent response is where pore pressures are generated when the cyclic stress level becomes zero ( $q_c = 0$ ), at the completion of each cycle of loading. The magnitude of these pore pressures is a function of the load, stress history and time. These pore pressures remain 'permanent' until the samples are allowed to drain. When the accrued pore pressure dissipates, it will be accompanied by a volume change, termed 'recompression' or 'reconsolidation', that is a function of the magnitude of permanent pore pressure. This in turn will give an additional settlement to the foundation soil. Due to this settlement, it is generally agreed that this permanent pore pressure response is an important criterion when dealing with non-failure cyclic loading situations.

The variations of pore pressure at peak compression and peak extension with time are presented in Figs 5 to 8. Each sample is represented by two lines; the upper line is the peak pore water pressure measured at the maximum cyclic stress level in compression and the lower line is the pore pressure measured at the maximum cyclic stress level in extension.

For normally consolidated samples, all samples except IRS012VL, generated positive pore pressure both at peak compression and peak extension throughout the test. However, for overconsolidated samples, all produced negative pore pressure at peak extension stress, during the early stage of cyclic loading. After cycling for two hours, the pore pressure eventually becomes positive. This was achieved at a shorter time for lightly overconsolidated samples (OCR 2). The amount of negative pore pressure developed also depends on the cyclic stress level. In OCR 2 samples, a pore pressure of -4 kPa was developed at a cyclic stress level of  $0.11p'_e$ , but an enormous -45 kPa at a cyclic stress level of  $0.256p'_e$ . The same trend is also observed in samples of OCR 4.

Figs. 5 to 8 also show that the pore water pressure generated at peak cyclic deviator stress in compression is always larger than that measured at peak extension. It is also observed that the magnitude increased with cyclic stress level. This can be seen clearly by examining the plots of cyclic pore pressure with time, as shown in Figs. 9 to 11. The  $A_c$  values tabulated in Table 3 however, show little variation with stress level and stress history. By eliminating the extreme values in the upper and lower bounds, i.e. results from Test IRS012L and IRS01B, the average of  $A_c$  for normally consolidated samples is found to be 0.26. For overconsolidated samples,  $A_c$  is 0.31 for OCR 2, and 0.33 for OCR 4. The results compare well with Raybould [5]. The  $A_c$  values for overconsolidated samples are greater, demonstrating the fact that overconsolidated samples generate higher cyclic pore pressure than normally consolidated samples.

The development of permanent pore water pressure with time is plotted in Figs. 12 to 14 for samples of OCR 1, 2 and 4, respectively. The pore pressure develops steadily with the loading period and it is observed that the rate of development decreases as the loading period increases. The magnitude of pore pressure increases with cyclic stress level for samples of the same stress history. However, given the same stress level, normally consolidated samples seem to generate higher permanent pore pressure than the overconsolidated samples at any time. This can be seen from a comparison of Figs. 12(c), 13(b) and 14(b), when the pore pressures are normalised with respect to the equivalent pressures,  $p'_e$ , i.e. the value of  $p'$  at the point on the normal consolidation line at the same specific volume. Therefore, it can be concluded that for overconsolidated samples, the rate at which permanent pore pressures built up was low compared to that for the normally consolidated samples.

Ward [21] and Conn [13] found that there is a linear relationship between the normalised pore pressure rate,  $u/p'_e$ , and the number of cycles,  $N$ , when the data are plotted on logarithmic scales. Hyde and Ward [12] showed that pore pressure development was independent of frequency.

The normalised permanent pore pressure rates are therefore plotted against time,  $t$ , instead of  $N$ , as shown in Figs. 15 to 17. Hyde et. al. [14] also presented their results in this way.

As expected, a linear relationship exists between  $\ln \frac{\dot{u}}{p'_e}$  and  $\ln t$ . The relationship between  $\frac{\dot{u}}{p'_e}$  and  $t$  can be expressed as :

$$\frac{\dot{u}}{p'_e} = bt^\beta \quad (2)$$

where

- $\dot{u}$  - the permanent excess pore water pressure developed per unit time
- $p'_e$  - the equivalent pressure
- $b$  - notional normalised pore pressure rate at unit time (1 second)
- $\beta$  - the gradient of the  $\ln \frac{\dot{u}}{p'_e} - \ln t$  plot, known as a 'decay' constant

Examination of Figures 15 to 17 showed no consistent trend for the variation of the slope  $\beta$  with cyclic stress level. The solid lines show the results of a linear regression carried out on all the data points at each stress history. The slope of this line in each case was then taken as the slope for all cyclic stress levels. From a comparison Figs. 15 to 17, it can be seen that  $b$  is a function of stress history and cyclic stress level. For each stress history,  $b$  increased with cyclic stress level. Using Equation (2), allowed the development of a pore pressure model which has been discussed by Marto [17] elsewhere.

### Cyclic Stress Path

The critical state boundary surface of the investigated material has been developed from the results of monotonic undrained compression and extension tests on isotropically and anisotropically consolidated samples of various stress histories [22]. Results of the pore pressure response could be shown within this boundary surface. However, as it is not possible to show the complete effective stress path for the cyclic loading tests owing to the large number of cycles involved, the cyclic effective stress paths are represented by drawing the applied stress path and showing the movement of  $p'/p'_e$  at the peak values of  $q/p'_e$ , as the pore pressures develop. The effective stress paths for non-failure samples are presented in Figs. 18 to 20.

If one initially considers the isotropically normally consolidated samples, the stress paths can all be seen to originate at  $p'/p'_e = 1.0$ . It is also observed that large positive pore pressures were developed, resulting in movement of the stress path towards the no-tension boundary [23]. The amount of pore pressure developed increased with the level of the applied cyclic stress, thus, a sample subjected to the highest cyclic stress level, has a stress path nearest to the no-tension boundary. The overconsolidated samples in this research can be considered as lightly overconsolidated and therefore also generated significant positive pore pressures, though these were of a lower magnitude than those observed for the normally consolidated samples. The stress paths, which started at  $p'/p'_e < 1.0$ , also moved to the left of the total stress path but remained well below the boundary surface.

## CONCLUSIONS

The following conclusions were drawn from the studies:

1. Positive pore pressures were generated at both peak compression and peak extension for normally consolidated samples. The pore pressures generated at peak compression were always larger than at peak extension. For overconsolidated samples, negative pore pressures were generated at peak extension, at the beginning of the test.
2. The cyclic pore pressure response varied with applied cyclic load and stress history. The parameter  $A_c$ , i.e. the ratio of cyclic pore pressure to cyclic deviator stress, can be used to describe the response.
3. The permanent pore pressure developed steadily with the loading period, but the rate of development decreased as the loading period increased. A linear relationship was found to exist between the normalised permanent pore pressure rate and time, plotted on logarithmic scales.
4. The development of permanent pore pressure moved the stress paths to the left of the total stress path but remained well below the critical state boundary surface of the silt material.

## REFERENCES

- [1] Koutsoftas, D.C., Effect of Cyclic Loads on Undrained Strength of Two Marine Clays, *ASCE Journal of Geotechnical Engineering Division*, Vol 104, No GT5, pp. 609 – 620, 1978.
- [2] Brown, S.F., Andersen, K.H. and McElvaney, J. The Effect of Drainage on Cyclic Loading of Clay, *Proc. 9th Int. Conf. on Soil Mechanics and Foundation Engineering*, Tokyo, Japan, pp. 195 – 200, 1977.

- [3] Yasuhara, K., Cyclic Strength and Deformation of Normally Consolidated Clay, *Japanese Society of Soil Mechanics and Foundation Engineering*, Vol. 22, No 3, 78 – 91, 1982.
- [4] Andersen, K.H., Brown, S.F., Foss, I., Pool, J.H. and Rosenbrand, W.F., Effect of Cyclic Loading on Clay Behaviour, *Proc. Conf. on Design and Construction of Offshore Structures*, Institute of Civil Engineers, pp. 75 – 79, 1976.
- [5] Raybould, M., *The Response of Silt-Clay Mixtures to Cyclic Loading*, PhD. Thesis, University of Nottingham, UK, 1991.
- [6] ASCE The Committee on Soil Dynamics of the Geotechnical Engineering Division, Definition of Terms Related to Liquefaction, *ASCE Journal of Geotechnical Engineering Division*, Vol. 104, No GT9, pp. 1197 – 1200, 1978.
- [7] Wood, D.M., Laboratory Investigations of the Behaviour of Soils under Cyclic Loading : A Review, Chapter 20, *Soil Mechanics - Transient and Cyclic Loads*, G.N. Pande and O.C. Zienkiewicz, Eds., John Wiley and Sons Ltd., pp. 513 – 582, 1982.
- [8] Airey, D.W. and Fahey, M., Cyclic Response of Calcareous Soil From the North-West Shelf of Australia, *Geotechnique* 41, No 1, pp. 101 – 121, 1982.
- [9] Sangrey, D.A. (1978). Marine Geotechnology - State of the Art, *Marine Geotechnology*, Vol 2, 45 - 80.
- [10] Lee, K.L. and Focht, J.A., Cyclic Testing of Soil for Ocean Wave Loading Problems, *Marine Geotechnology*, Vol 1, No 4, pp. 305 – 325, 1976.
- [11] Wilson, N.E. and Greenwood, J.R., Pore Pressures and Strains after Repeated Loading of Saturated Clay, *Canadian Geotechnical Journal*, Vol 11, No 2, pp. 269 – 277, 1974.
- [12] Hyde, A.F.L. and Ward, S.J., A Pore Pressure and Stability Model for a Silty Clay under Repeated Loading, *Geotechnique* 35, No 2, pp. 113 – 125, 1985.
- [13] Conn, G.M., *The Two-Way Repeated Loading of a Silty Clay*, PhD. Thesis, Loughborough University of Technology, UK, 1988.
- [14] Hyde, A.F.L., Yasuhara, K. and Hirao, K., Stability Criteria for Marine Clay under One-way Cyclic Loading, *ASCE Journal of Geotechnical Engineering Division*, Vol. 119, No 11, pp. 1771 – 1789, 1993.



- [15] Taylor, P.W. and Bacchus, D.R., Dynamic Cyclic Strain Tests on a Clay, *7th European Conference on Soil Mechanics and Foundation Engineering*, Vol 1, pp. 401 – 410, 1969.
- [16] Sangrey, D.A., Henkel, D.J. and Esrig, M.I., The Effective Stress Response of a Saturated Clay Soil to Repeated Loading, *Canadian Geotechnical Journal*, Vol. 6, pp. 421 – 430, 1969.
- [17] Marto, A., Pore Pressure Model of Undrained Two-Way Cyclic Loading of Silt, *4<sup>th</sup> Regional Conference in Geotechnical Eng. (GEOTROPIKA '97)*, Malaysia, pp. 123 – 142, 1997.
- [18] Hyde, A.F.L, Marto, A and Yasuhara, K., Volumetric Compression of Periodically Loaded Silt, *International Conference on Deformation and Progressive Failure in Geomechanics*, Nagoya, Japan, 1997.
- [19] Menzies, S., A Computer Controlled Hydraulic Triaxial Testing System, *Advanced Triaxial Testing of Soil and Rock*, ASTM STP 977, 82 – 94, 1988.
- [20] Marto, A., *Volumetric Compression of a Silt under Periodic Loading*, PhD. Thesis, University of Bradford, U.K, 1996a.
- [21] Ward, S.J., *The Stability of a Silty Clay under Repeated Loading*, PhD. Thesis, Loughborough University of Technology, UK, 1983.
- [22] Marto, A., Critical State of Keuper Marl Silt, *Civil Engineering Journal*, Faculty of Civil Engineering, UTM, Vol. 9 No 2, pp. 34 – 58, 1996b.
- [23] Wood, D.M., *Soil Behaviour and Critical State of Soil Mechanics*, Cambridge University Press, 1990.

Table 1 Two-way Cyclic Loading Tests (without rest-periods)

Test Number	OCR	Mean Normal Effective Stress, $p'$ (kPa)	Cyclic Stress Level, $q_c$ $\pm$ (kPa)	Normalised Cyclic Stress Level, $q_c/p'_e$ $\pm$	Remarks
ISS011	1	600	0.25 $q_f$ (108.8)	0.181	10 cycles
ISS013	1	600	0.5 $q_f$ (217.7)	0.363	10 cycles
ISLA12	1	400	0.25 $q_f$ (68)	0.163	100 cycles
ISL012	1	600	0.25 $q_f$ (108.8)	0.185	100 cycles
ISL022	2	300	0.25 $q_f$ (93.06)	0.175	100 cycles
ISL042	4	150	0.25 $q_f$ (78.61)	0.188	100 cycles

Table 2 Two-way Cyclic Loading Tests with Rest-Periods

Test Number	OCR	Mean Normal Eff. Stress, $p'$ (kPa)	Cyclic Stress Level, $q_c$ $\pm$ (kPa)	Cyclic stages
IRSA1B	1	400	0.15 $q_f$ (40.8)	3
IRSA12	1	400	0.25 $q_f$ (68)	3
IRSA1A	1	400	0.35 $q_f$ (95.2)	3
IRS01B	1	600	0.15 $q_f$ (65.3)	3
IRS012	1	600	0.25 $q_f$ (108.8)	3
IRS01A	1	600	0.35 $q_f$ (152.4)	3
IRS02B	2	300	0.15 $q_f$ (55.84)	3
IRS022	2	300	0.25 $q_f$ (93.06)	3
IRS02A	2	300	0.35 $q_f$ (130.3)	3
IRS04B	4	150	0.15 $q_f$ (47.17)	3
IRS042	4	150	0.25 $q_f$ (78.61)	3
IRS012L	1	600	0.25 $q_f$ (108.8)	6
IRS042L	4	150	0.25 $q_f$ (78.61)	6
IRS012VL	1	600	0.25 $q_f$ (108.8)	1
IRS022VL	2	300	0.25 $q_f$ (93.06)	1
IRS042VL	4	150	0.25 $q_f$ (78.61)	1

Table 3 Cyclic pore pressure parameter,  $A_c$

Test No	OCR	$\Delta u_c$ (kPa)	Pore Pressure Parameter, $A_c$
IRSA1B	1	20.76	0.254
IRSA12	1	31.53	0.232
ISLA12	1	40.01	0.294
IRSA1A	1	45.20	0.237
IRS01B	1	21.50	0.165
IRS012	1	61.35	0.282
ISL012	1	44.07	0.203
IRS012L	1	84.10	0.386
IRS012VL	1	64.70	0.297
IRS01A	2	76.52	0.250
IRS02B	2	32.60	0.292
ISL022	2	53.03	0.285
IRS022VL	2	6.28	0.361
IRS022	2	44.90	0.241
IRS02A	2	90.08	0.346
IRS04B	4	30.30	0.321
IRS042	4	58.93	0.375
ISL042	4	43.51	0.277
IRS042L	4	54.01	0.344
IRS042VL	4	55.27	0.352

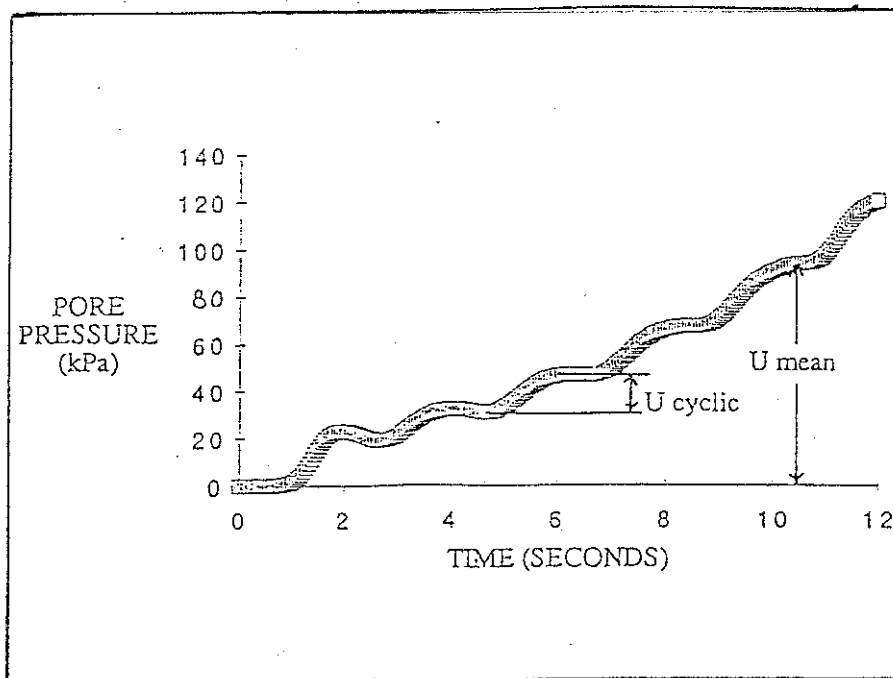
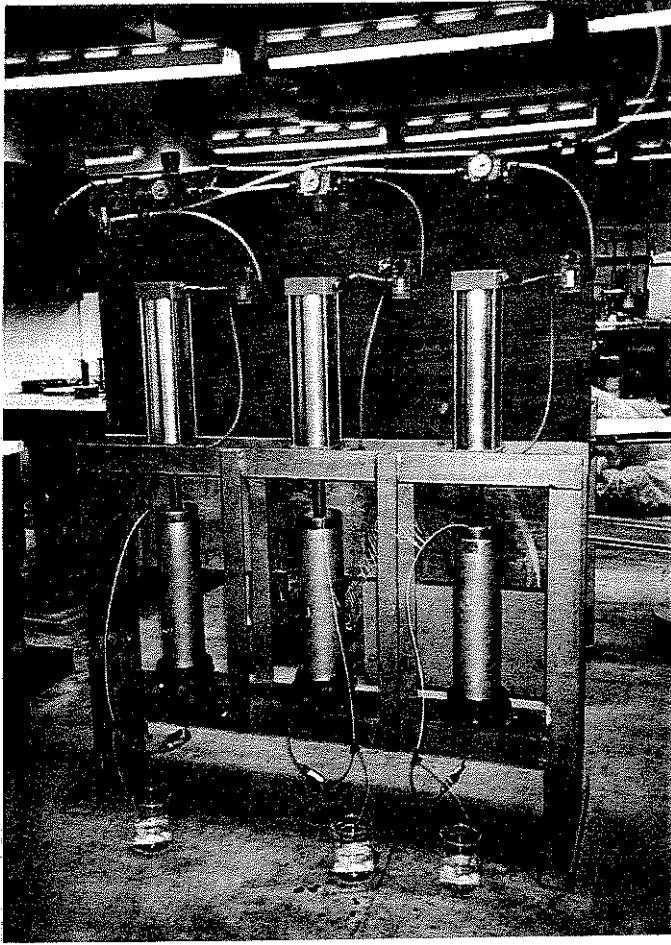
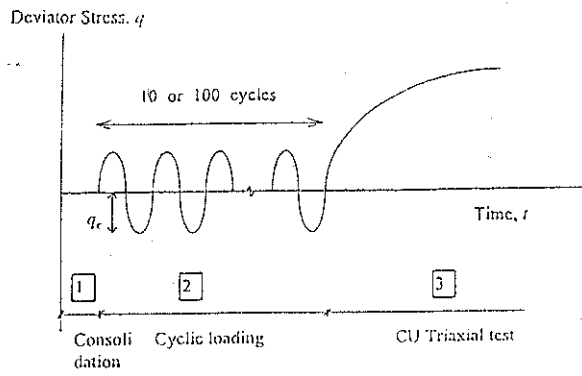
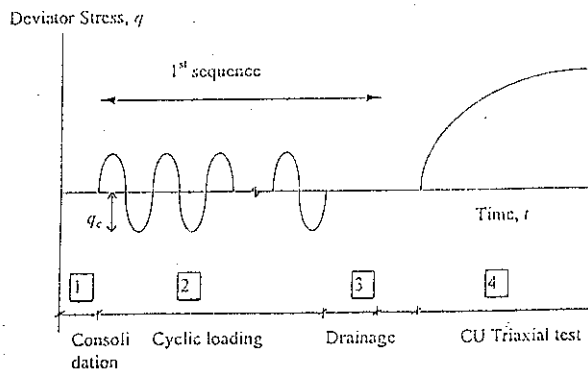


Figure 1 Pore pressure response to two-way cyclic loading (after Raybould [5])





(a) Cyclic loading without rest-periods



(b) Cyclic loading with rest-periods

Figure 3 Loading sequence in cyclic test series

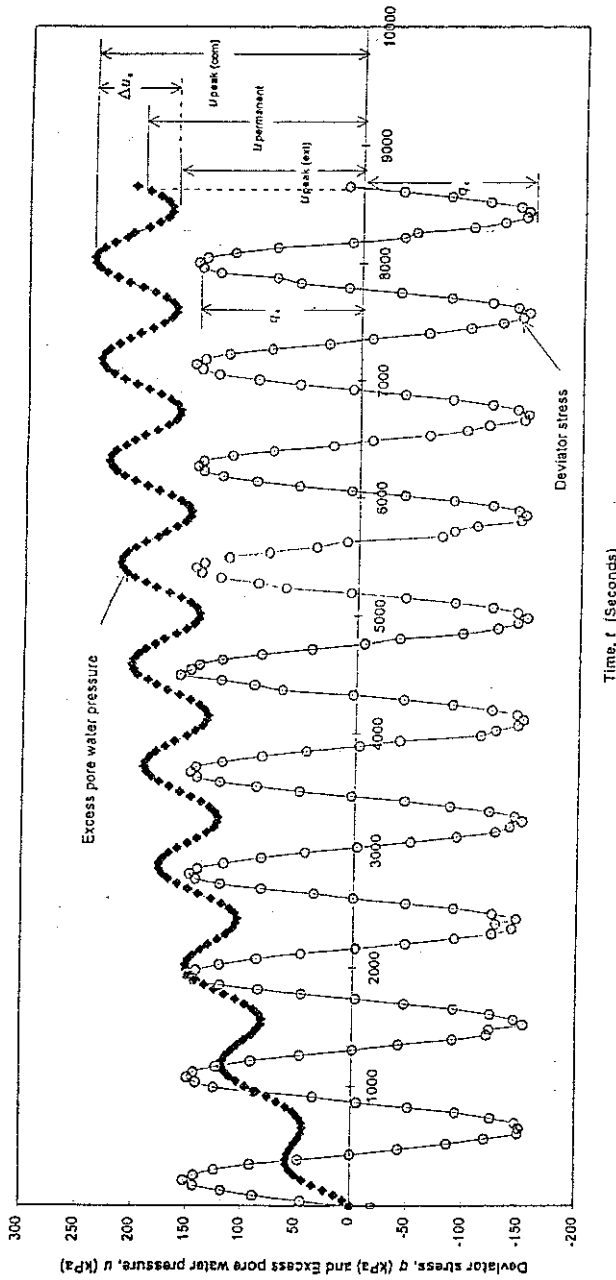
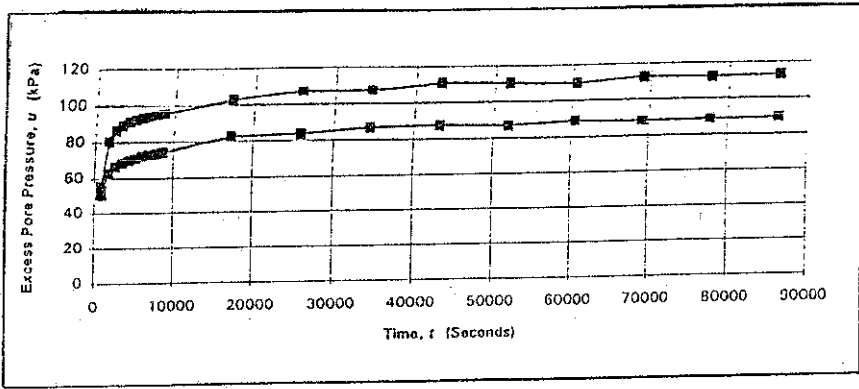
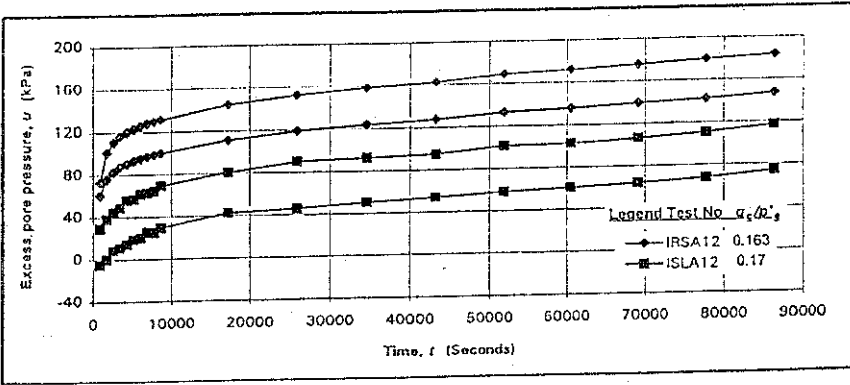


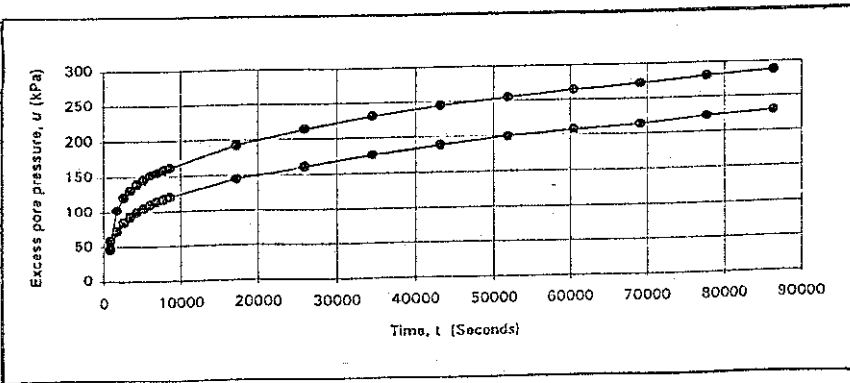
Figure 4 Pore pressure response to undrained two-way cyclic loading  
(Test No IRS01A)



(a)  $q_c/p'_e = 0.102$

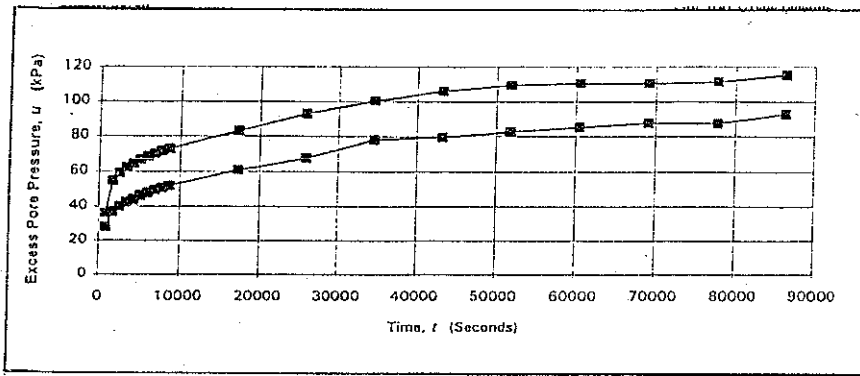


(b)  $q_c/p'_e = 0.163$  and  $0.17$

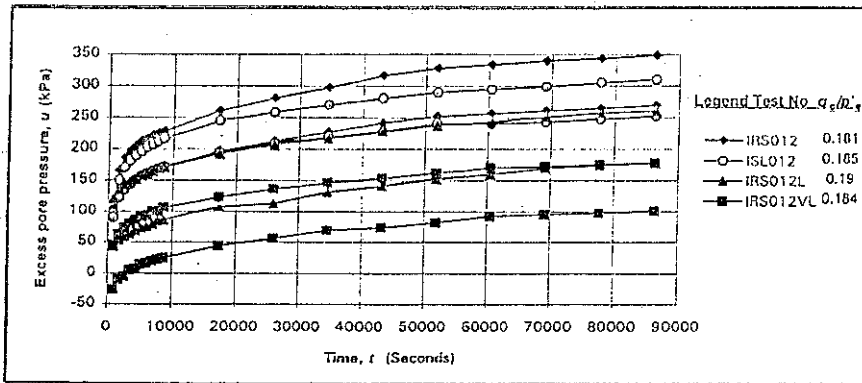


(c)  $q_c/p'_e = 0.238$

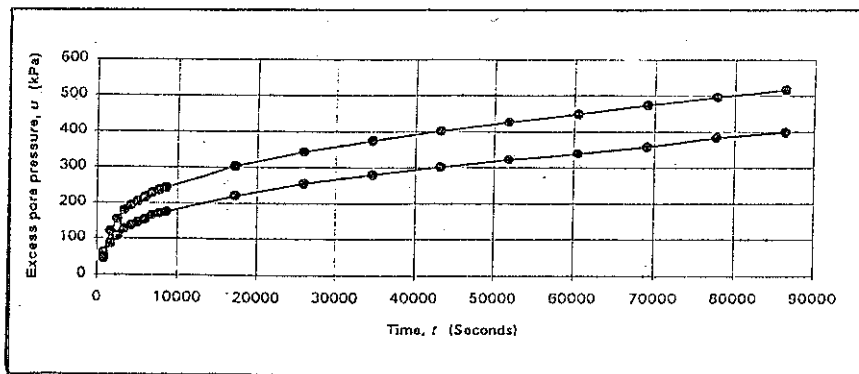
Figure 5 Excess pore water pressure (peak) versus time  
(OCR 1,  $p' = 400$  kPa)



(a)  $q_c/p'_e = 0.109$



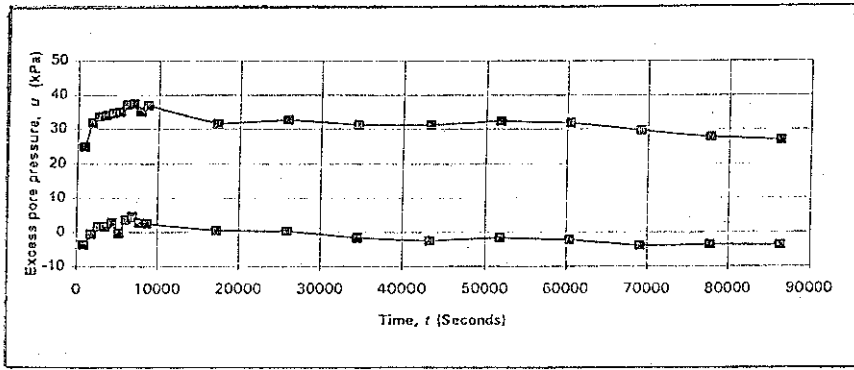
(b)  $q_c/p'_e = 0.181$  to  $0.19$



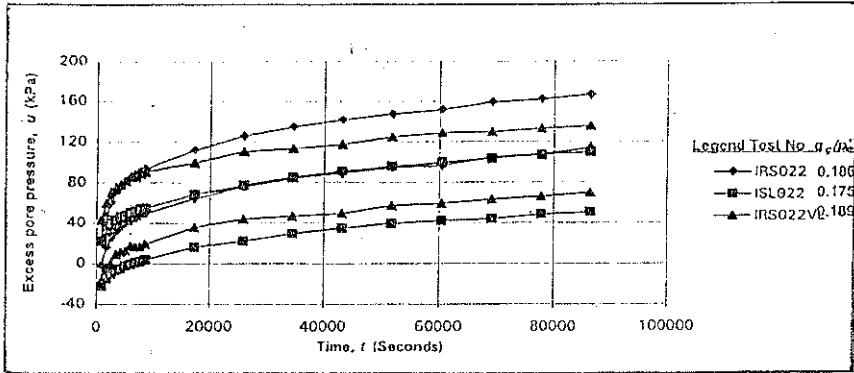
(c)  $q_c/p'_e = 0.254$

Figure 6 Excess pore water pressure (peak versus time  
(OCR 1,  $p' = 600$  kPa))

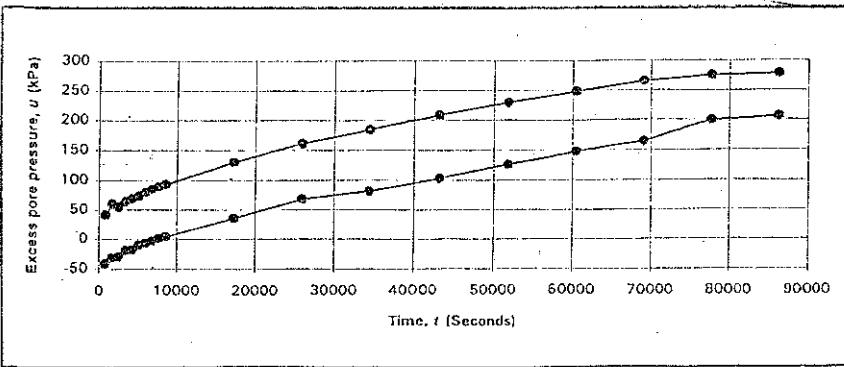




(a)  $q_c/p'_e = 0.111$

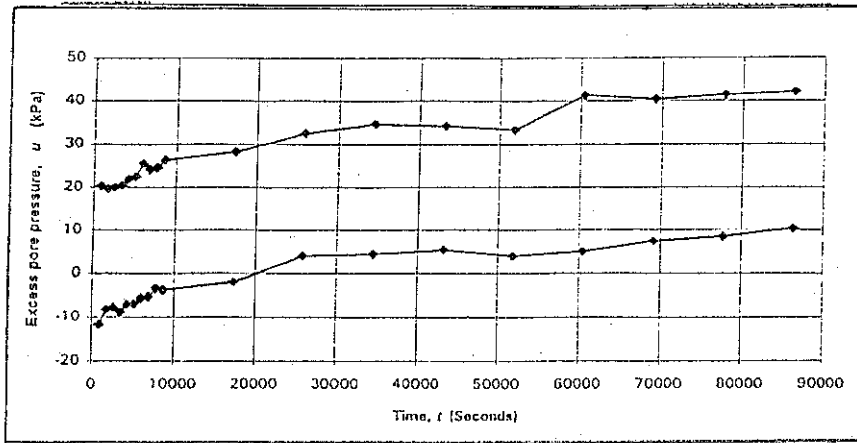


(b)  $q_c/p'_e = 0.175$  to  $0.189$

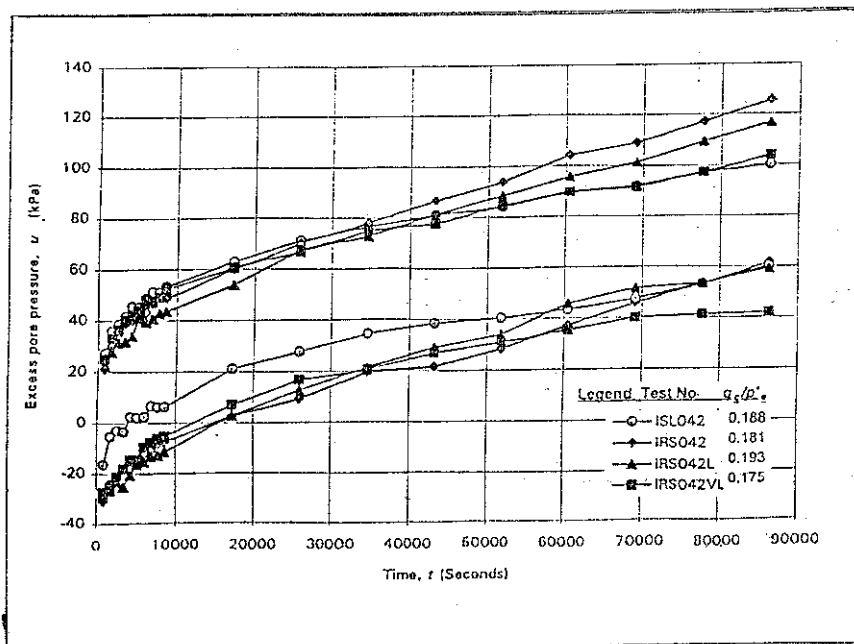


(c)  $q_c/p'_e = 0.256$

Figure 7 Excess pore water pressure (peak versus time (OCR 2))

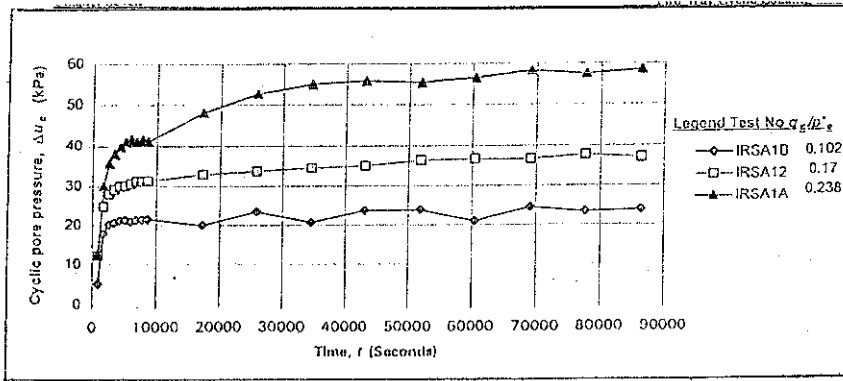


(a)  $q_c/p'_e = 0.11$

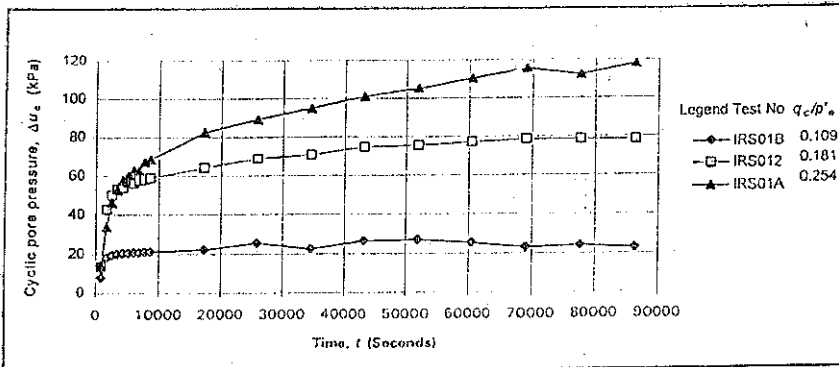


(a)  $q_c/p'_e = 0.175$  to  $0.193$

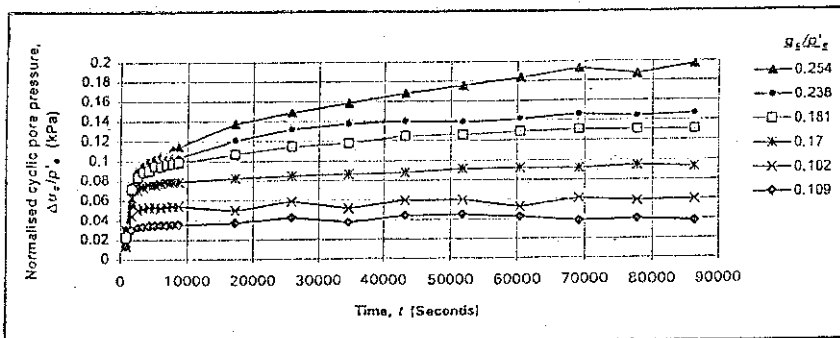
Figure 8 Excess pore water pressure (peak versus time (OCR 4))



(b)  $p' = 400$  kPa

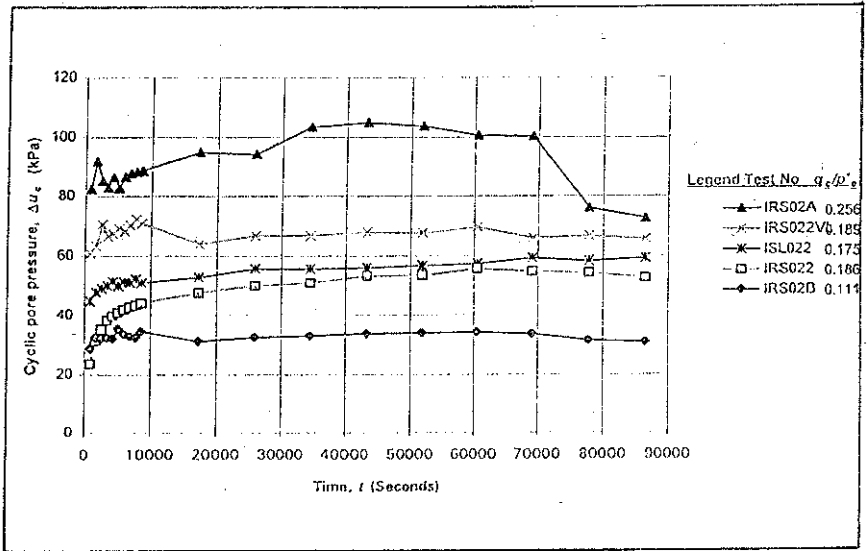


(b)  $p' = 600$  kPa

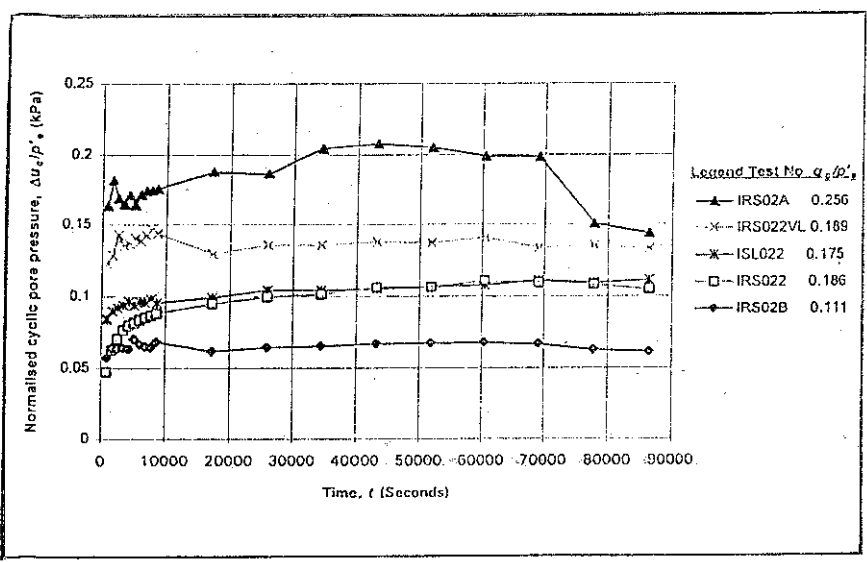


(c) Normalised cyclic pore pressure versus time, various stress levels

Figure 9 Cyclic pore water pressure versus time  
(OCR 1)

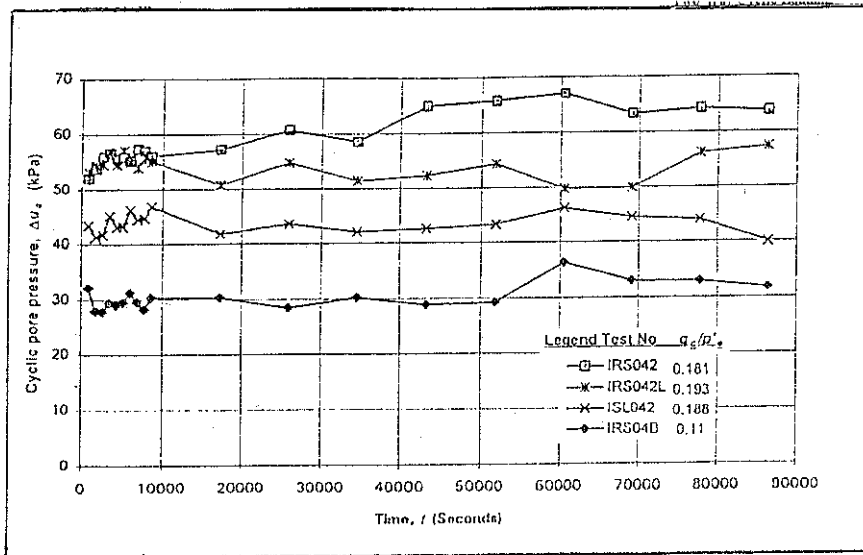


(a)

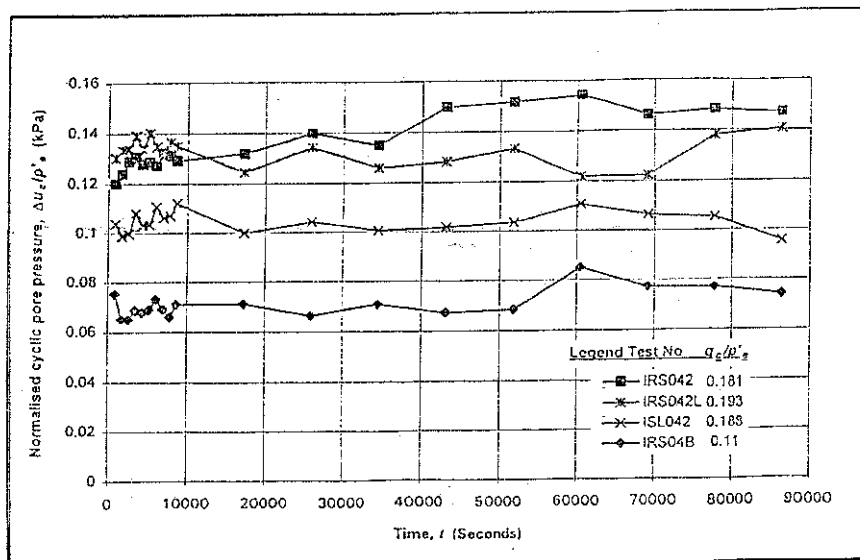


(b)

Figure 10 Cyclic pore water pressure versus time (OCR 2)

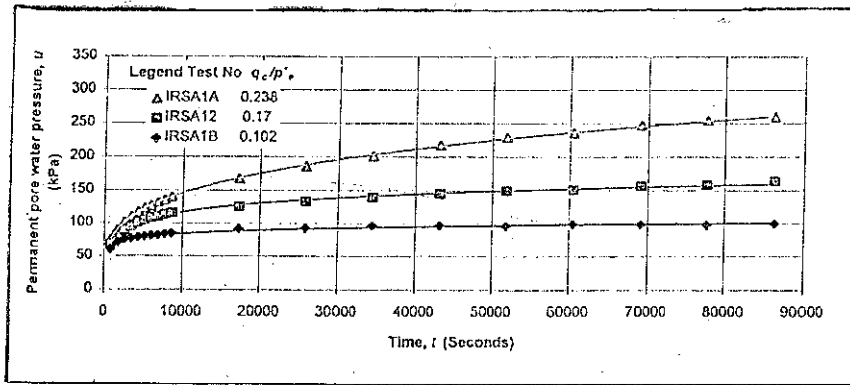


(a)

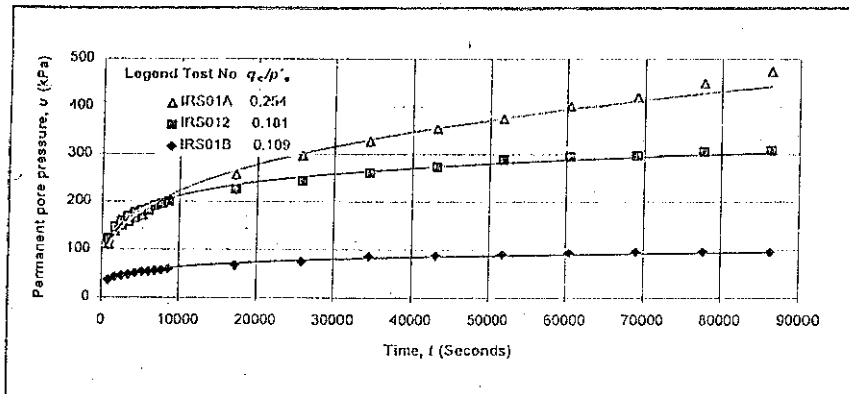


(b)

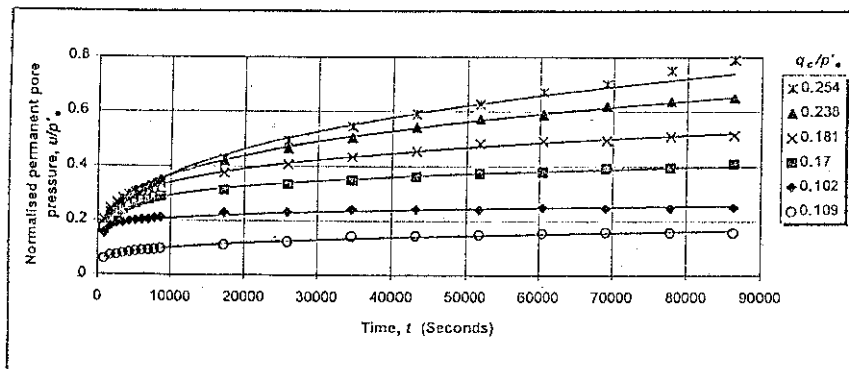
Figure 11 Cyclic pore water pressure versus time (OCR 4)



(a)  $p' = 400$  kPa



(b)  $p' = 600$  kPa



(c) Normalised permanent pore pressure versus time, various stress levels

Figure 12 Permanent pore water pressure versus time (OCR 1)

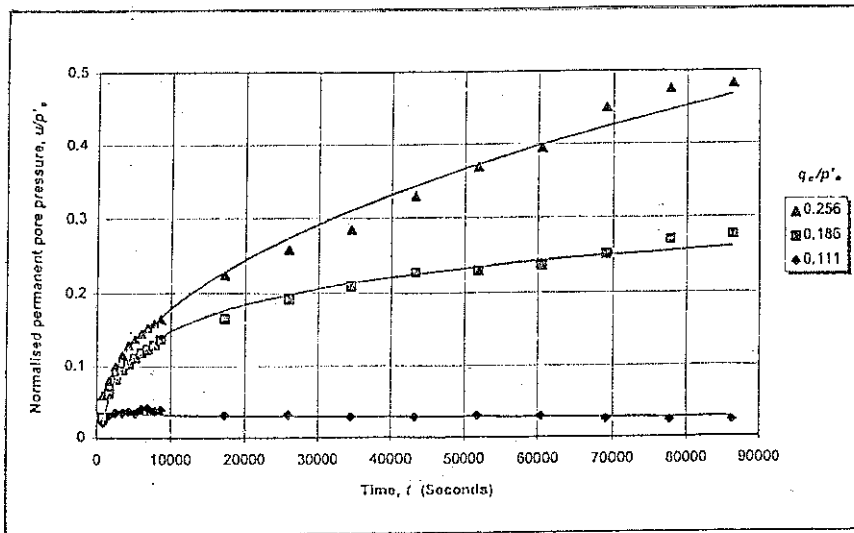
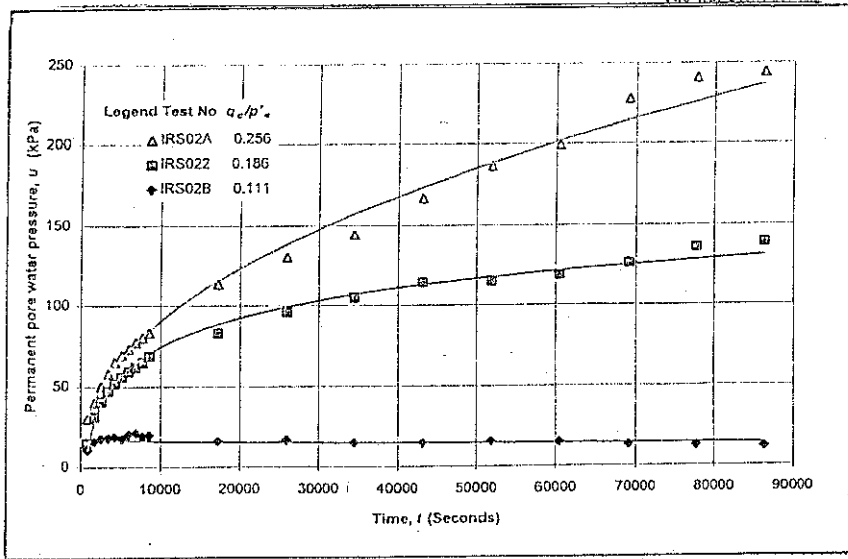


Figure 13 Permanent pore water pressure versus time (OCR 2)

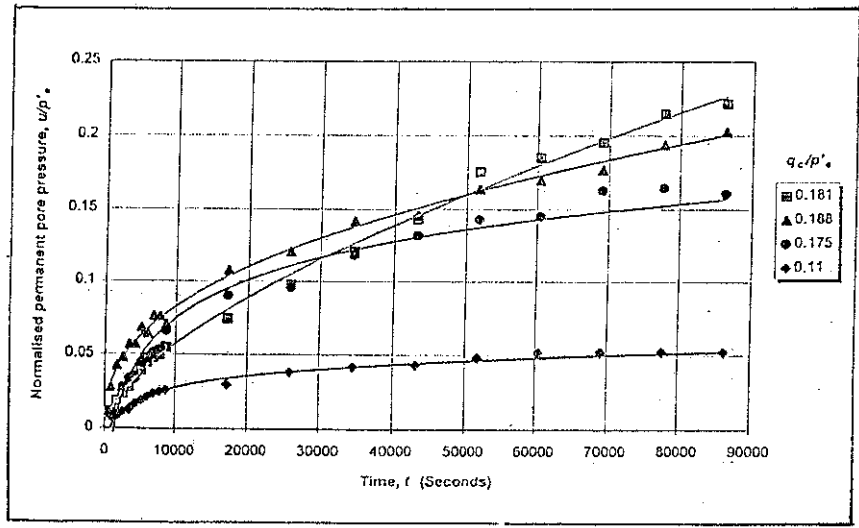
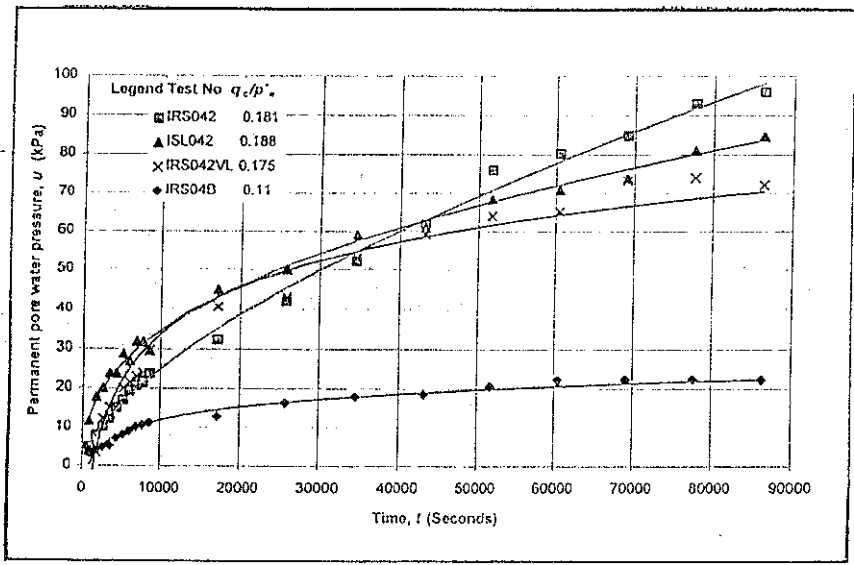


Figure 14 Permanent pore water pressure versus time (OCR 4)



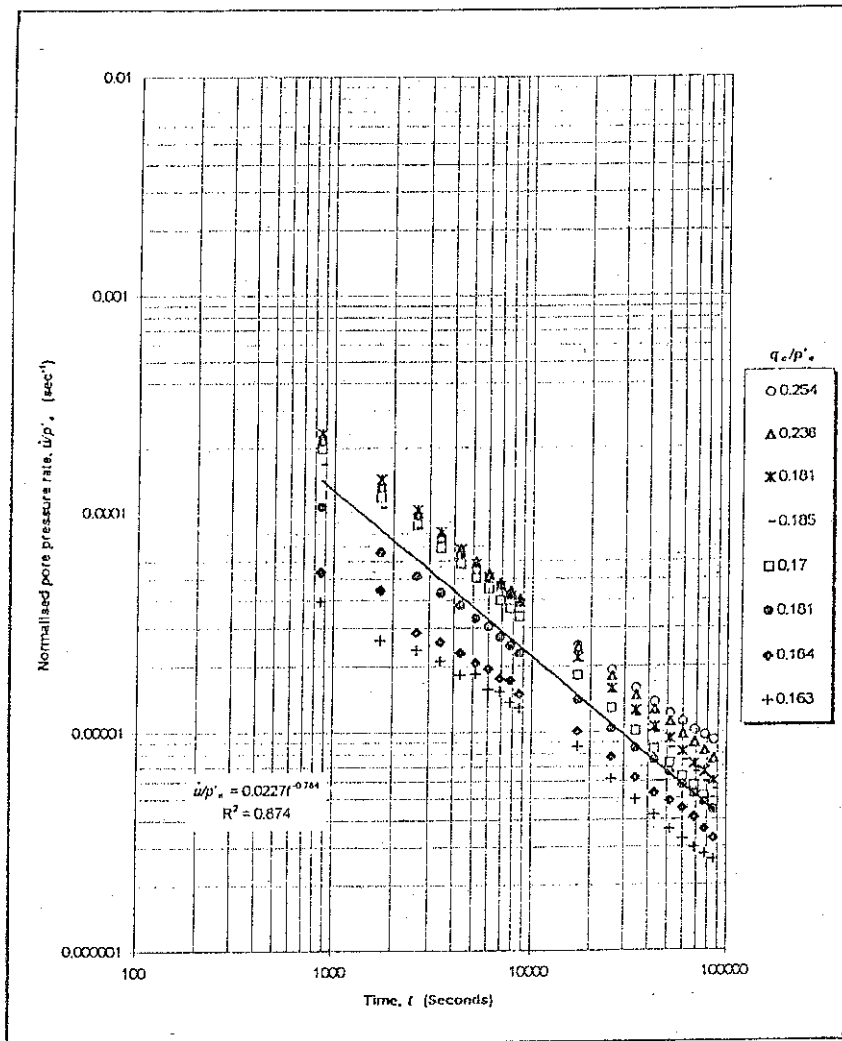


Figure 15 The relationship between  $\dot{u}/p'_e$  and time for OCR 1 at various  $q_e/p'_e$

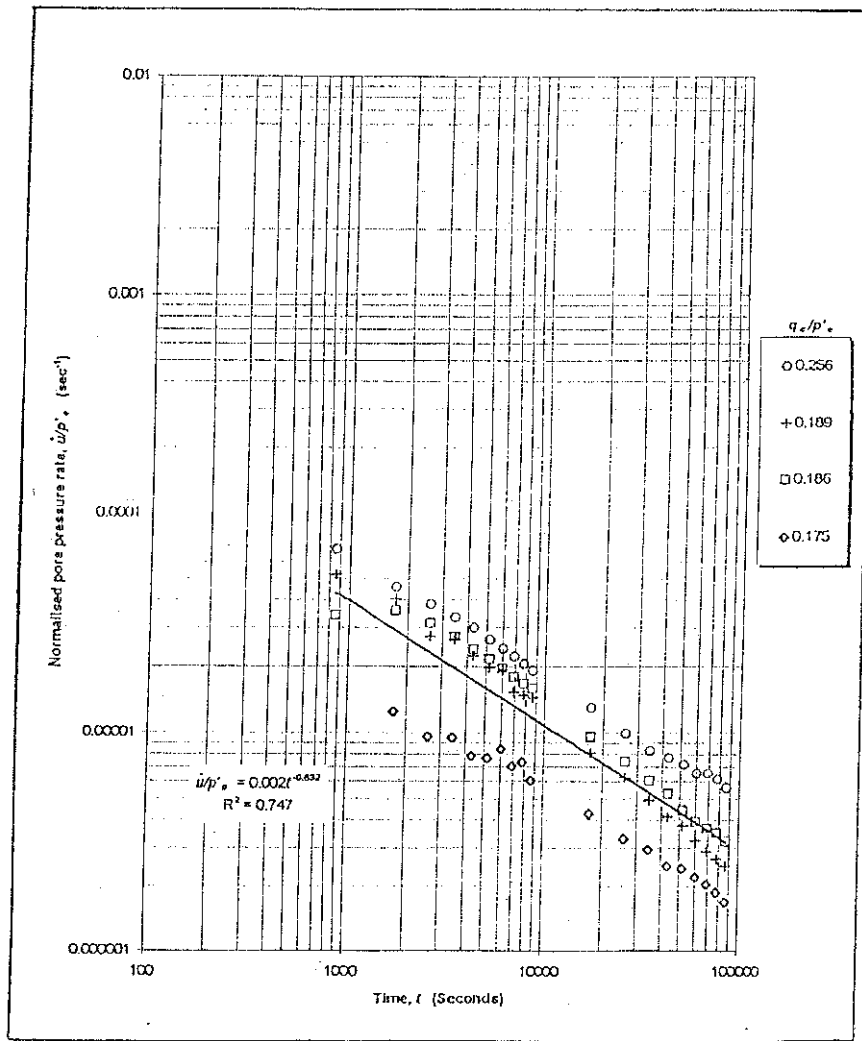


Figure 16 The relationship between  $u/p'_e$  and time for OCR 2 at various  $q_e/p'_e$

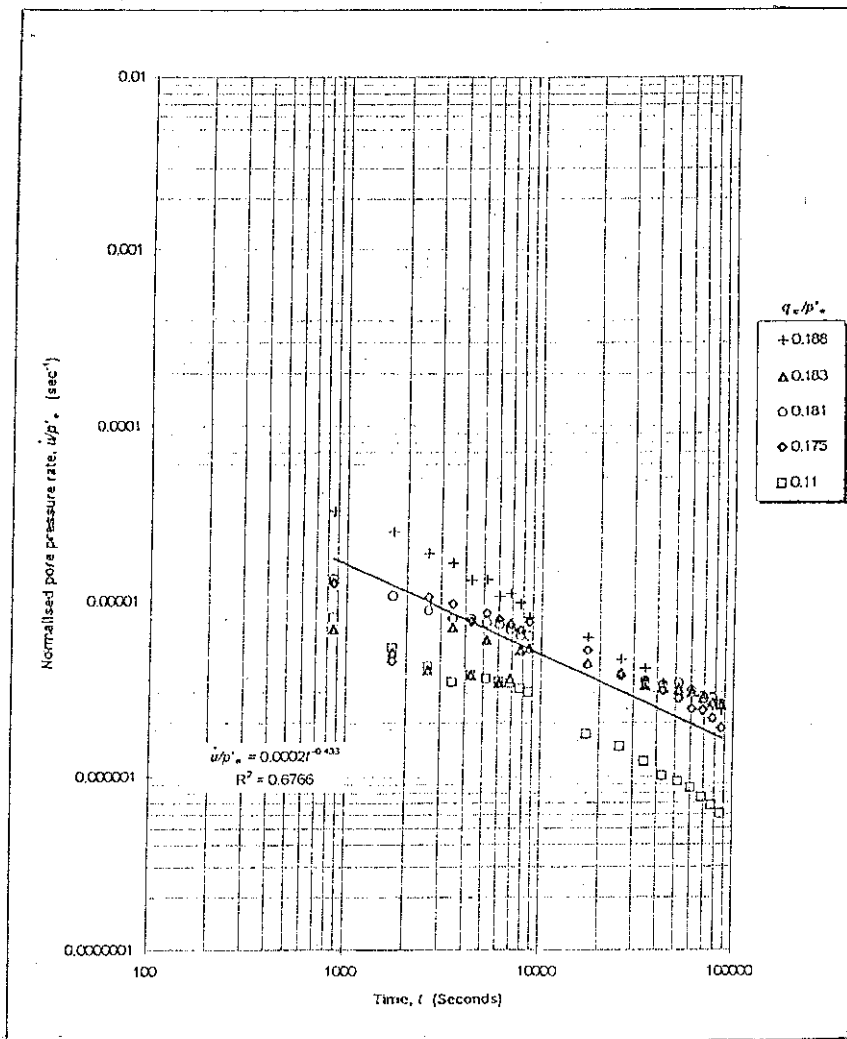


Figure 17 The relationship between  $u/p'_e$  and time for OCR 4 at various  $q_e/p'_e$

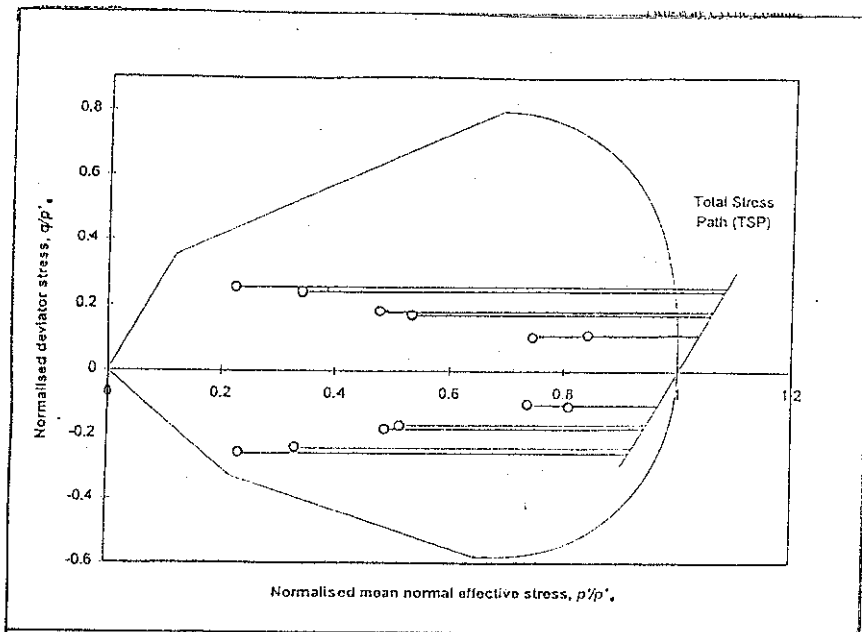


Figure 18 Cyclic stress paths for OCR 1

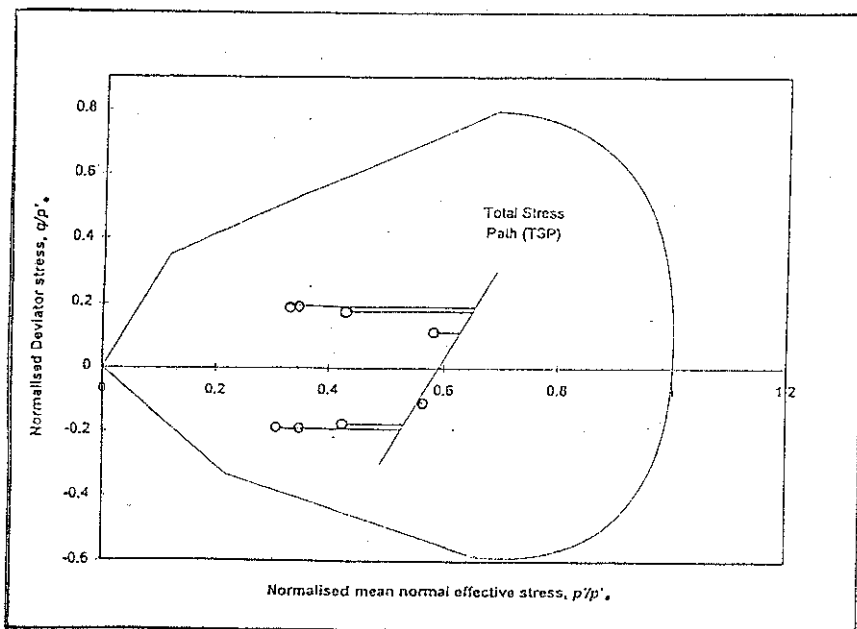


Figure 19 Cyclic stress paths for OCR 2

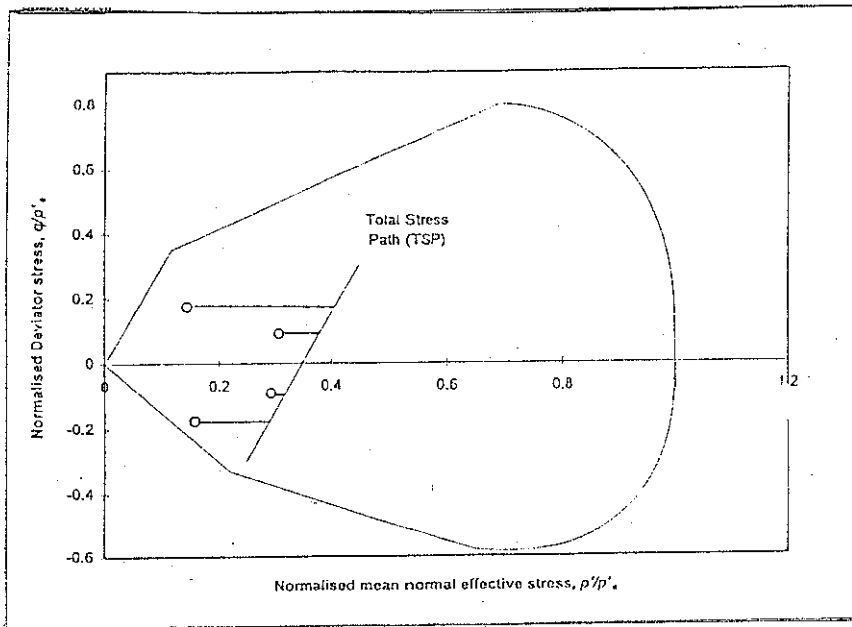


Figure 20 Cyclic stress paths for OCR 4